XII. PLASMA MAGNETOHYDRODYNAMICS AND ENERGY CONVERSION[*]

A. AN ELECTRODYNAMIC AMPLIFIER FOR A LOW-CONDUCTIVITY PLASMA

An electrodynamic amplifier for which compressible effects and the density of the surrounding medium could be ignored was considered by Melcher in the last report.[1] The theoretical part of this report is concerned with the study of a similar problem in which these effects are included in the analysis.

The model used for our device is shown in Fig. XII-1. A jet of plasma of low conductivity at ground potential travels along the axis of a cylindrical conductor with a voltage, V, with respect to the jet. Small surface perturbations are assumed in this analysis. In the experiment they are induced electrically by oscillator-amplifier combinations that are terminated in small spherical electrodes.

1. Analysis

From Maxwell's equations, the free-charge relaxation time constant is given by

$$T_r = \frac{\epsilon}{\sigma}. \tag{1}$$

If this time is much greater than a period of excitation, $\frac{1}{f}$, then the jet can be assumed to be chargefree. Thus we shall assume that

$$\sigma \gg f\epsilon. \tag{2}$$

Gravity, viscosity, and magnetic fields are neglected and the process is assumed to be isentropic. Thus the bulk equations are:

$$\rho\left[\frac{\partial \vec{V}}{\partial t} + (\vec{V}\cdot\nabla)\vec{V}\right] + \nabla p = 0 \tag{3}$$

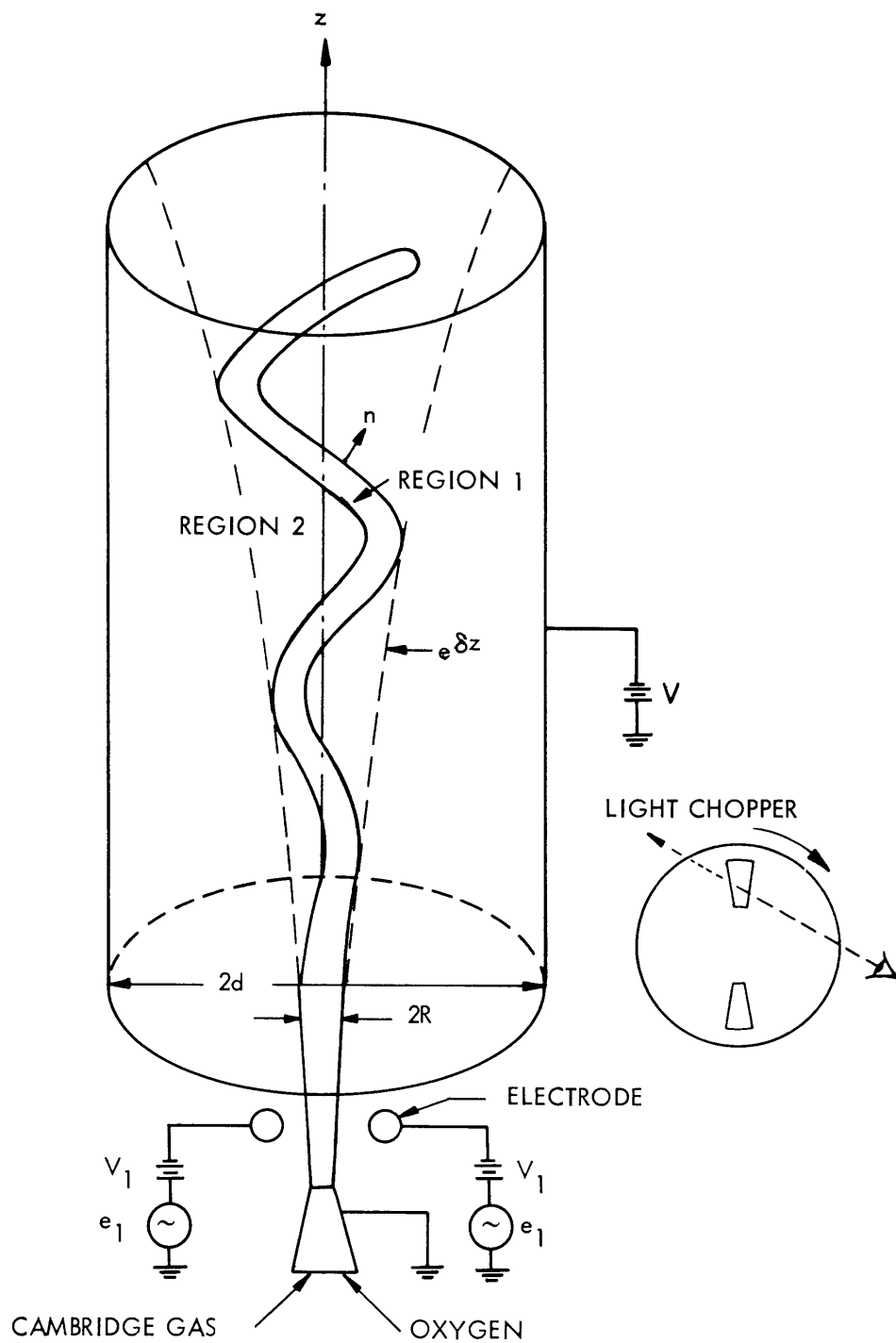Fig. XII-1. Diagram of the experiment.

$$\frac{\partial \rho}{\partial t} + \nabla \cdot (\rho \vec{V}) = 0 \tag{4}$$

$$\frac{Ds}{Dt} = 0 \tag{5}$$

$$\nabla \cdot \vec{E} = 0 \tag{6}$$

$$\nabla \times \vec{E} = 0, \tag{7}$$

where ρ and $\vec{V}$ are the fluid density and velocity, p is the pressure, s is the entropy, and $\vec{E}$ is the electric field.

Our analysis is similar to that used by Melcher and will not be repeated here. The complete analysis for this particular problem is given in the author's thesis.[2] The only modification to Melcher's work (in addition to the fact that compressibility and the density of the outer medium is considered) in this report is that the analogy between sheath energy and surface tension proposed by Rose and Clark, Jr.[3] is used. That is, the surface tension of the water jet, T, is replaced by S, the sheath energy of the plasma jet.

2. Dispersion Equation

If solutions of the form

$$\xi = \xi_0 + \xi' = \xi_0 + \hat{\xi}\, e^{j(\omega t + m\theta + kz)}, \tag{8}$$

where ξ is any one of the vector or scalar variables, are assumed, it is necessary to let

$$k = -\left(\frac{\omega}{v_z} + j\delta\right) \tag{9}$$

in order for the surface waves to amplify as they propagate in the positive z-direction with a phase velocity v_z. That is,

$$\exp[j(\omega t + m\theta + kz)] = \exp(\delta z)\, \exp\left[j\omega\left(t - \frac{z}{v_z}\right)\right] \exp(jm\theta). \tag{10}$$

With the restriction that

$$\delta \ll \frac{\omega}{v_z} \tag{11}$$

the dispersion equation becomes

$$-(\delta MR)^2 = \frac{M_c^2}{f(\beta R)}\left[\Gamma\left(1 + \frac{1}{L_m(\alpha)}\right) + \alpha^2 + m^2 - 1\right], \tag{12}$$

into which the following dimensionless parameters have been introduced:

167

Mach number

$$M = \frac{v_z}{c} \tag{13}$$

"Capillary Mach number" squared

$$M_c^2 = \frac{S}{R\rho_o^{(1)}c^2} \tag{14}$$

Normalized voltage squared

$$\Gamma = \frac{V'^2\epsilon}{RS} \tag{15}$$

Normalized frequency

$$\alpha = \frac{\omega R}{v_z}. \tag{16}$$

In Eq. 12

$$f(\beta R) = K_m(\beta R) - \frac{\rho_o^{(2)}}{\rho_o^{(1)}} L_m(\beta R) \tag{17}$$

$$K_m(x) = \frac{J_m(jx)}{j \, x \, J_m'(jx)} \tag{18}$$

$$L_m(x) = \frac{H_m(jx)}{j \, x \, H_m'(jx)} \tag{19}$$

$$\beta R \simeq \left[(\delta M R)^2 + \alpha^2\right]^{1/2} \tag{20}$$

$$V' = \frac{V}{\ln\left(\frac{d}{R}\right)}. \tag{21}$$

Here, H_m is the Hankel function of the first kind and J_m is the Bessel function, both being of order m; R is the radius of the jet; d, the radius of the electrode; ω, the angular frequency; k, the wave number; and m, the mode of propagation. The superscript numerals refer to regions (1) and (2), respectively.

3. Interpretation of Results

The IBM 7090 computer was used to solve the dispersion equation so that gain curves similar to Figs. XII-6 and XII-7 of Melcher's report could be obtained. The general shape of the curves is unchanged, but the gain is found to be a function of M_c for

the compressible case.

It is possible to plot a_m, the value of a for which a maximum in (δMR) occurs, as a function of Γ. (The δ' is analogous to δMR/M_c^2.) These plots are shown in Fig. XII-2
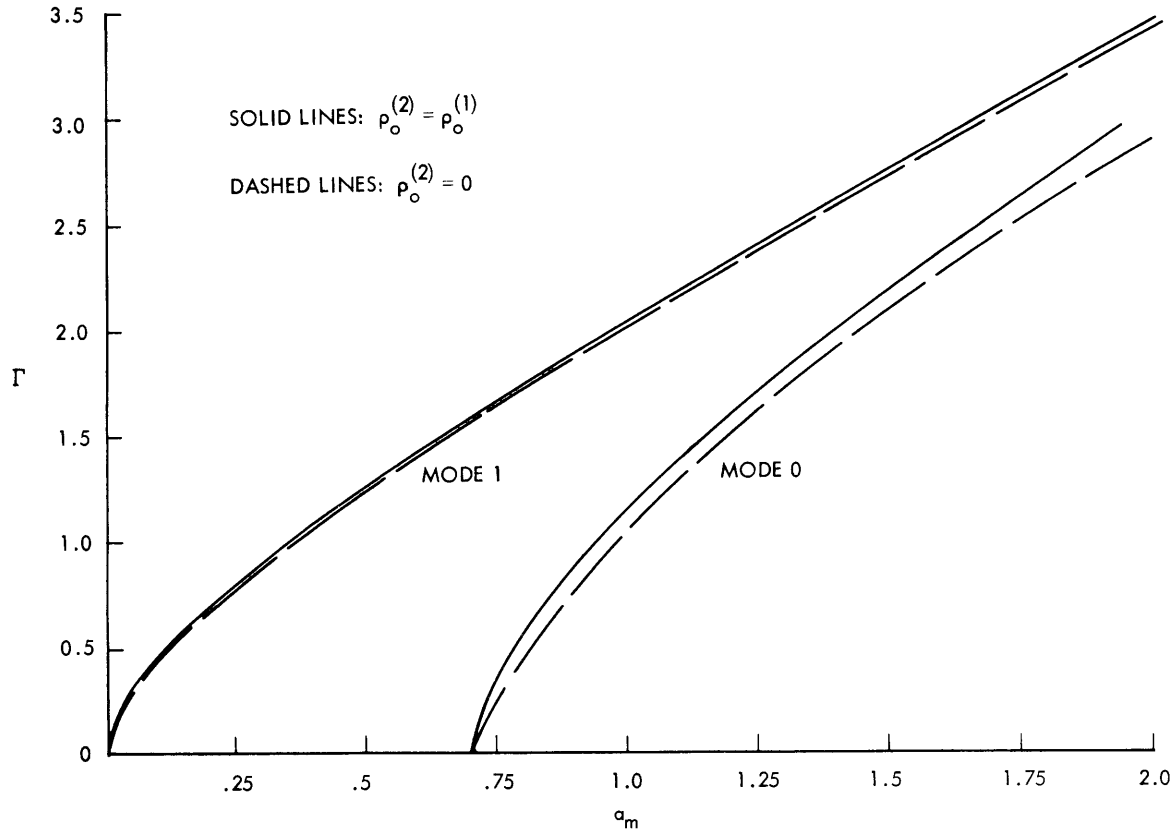

Fig. XII-2. Effect of $\rho_o^{(2)}$ on Γ vs a_m.

for the cases $\rho_o^{(2)} = 0$ and $\rho_o^{(2)} = \rho_o^{(1)}$. Note that the density of the outer medium alters a_m only slightly for a given Γ.

It was found theoretically that although M_c did affect the gain curves, it had no effect on a_m. That is, peak gain occurs for the same value of a (for a given Γ) independently of M_c. The IBM 7090 computer was used to obtain the optimization curves shown in Figs. XII-3 and XII-4. For each Γ = constant curve, the associated value of a_m is used for $\rho_o^{(1)} = \rho_o^{(2)}$. Thus knowing M_c and the amplifier voltage, V, which we want to use, we can use these curves to find the proper value of a to obtain maximum gain. M_c can be determined if S is known, and S can be experimentally determined.[2]

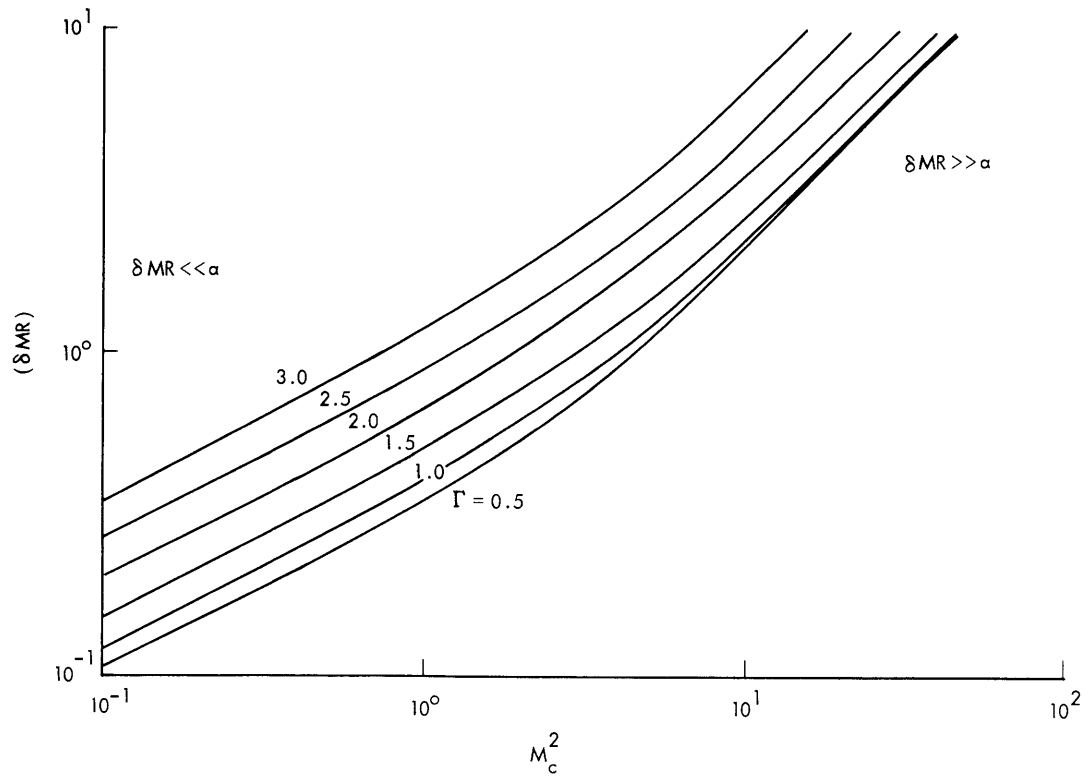In comparing this study with Melcher's, the main effects of compressibility were found to be:
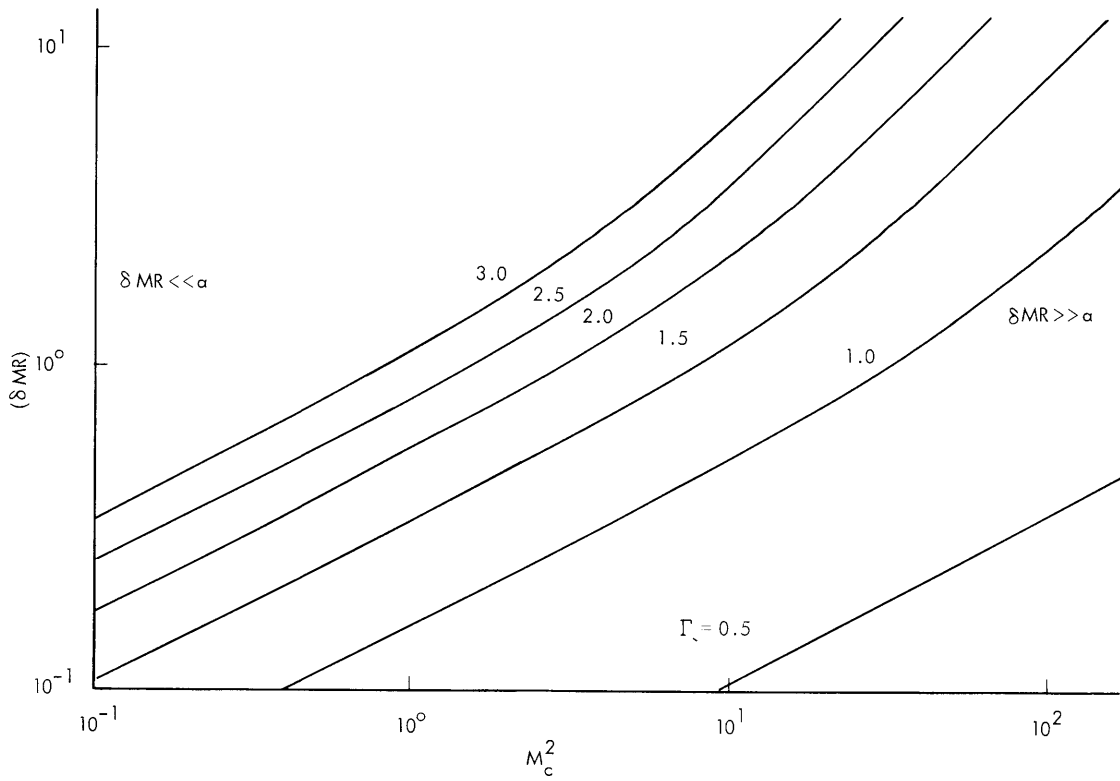
Fig. XII-3. Optimum operating conditions for Mode 0.

Fig. XII-4. Optimum operating conditions for Mode 1.

(a) The conditions for both gain and cutoff are independent of compressibility.

(b) δ must be sacrificed as M is increased (under the assumption that R is fixed) to remain at a given operating point on the gain curves (both δMR and a fixed).

(c) For a given value of Γ, the maximum value of (δMR) occurs for the same value of a_m, independently of compressibility.

(d) In the highly compressible region, δMR $\gg a$, the change in (δMR) for a given increase in M_c^2 is twice as great as the change in (δMR) for the same increase in M_c^2 in the incompressible region, (δMR) $\ll a$.

4. Experiment

The plasma used for the experiment was a natural gas-oxygen flame. Adjustments were made until the flame was blue, the estimated temperature being 1700°C. The radius and velocity were fixed at 0.75 cm and ~5 m/sec, respectively.

The two oscillator-amplifier combinations were adjusted to be 180° out of phase in order to excite mode 1. Two parallel brass plates were used instead of a cylindrical electrode as shown in Fig. XII-1 because it was found that reflections caused by any cylindrical structure made photographs ambiguous.

We found that in order for the surface waves to be amplified the exciter frequency had to be less than approximately 40 cps for the voltages used. Cutoff was observed when the exciter frequency was greater than this value. The working flame was only approximately 16 cm long, and consequently only one full wavelength could be observed on the jet.
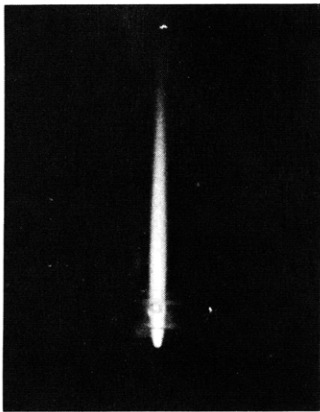

Fig. XII-5.   Excited flame with amplifier voltage = 0.

The surface waves were evident when the flame was observed through the light chopper because the flame was seen to be kinked when the amplifier voltage, V, was applied. However, no kinks were observed when the amplifier voltage was not applied.

That the surface waves did amplify was verified by desynchronizing the chopper and
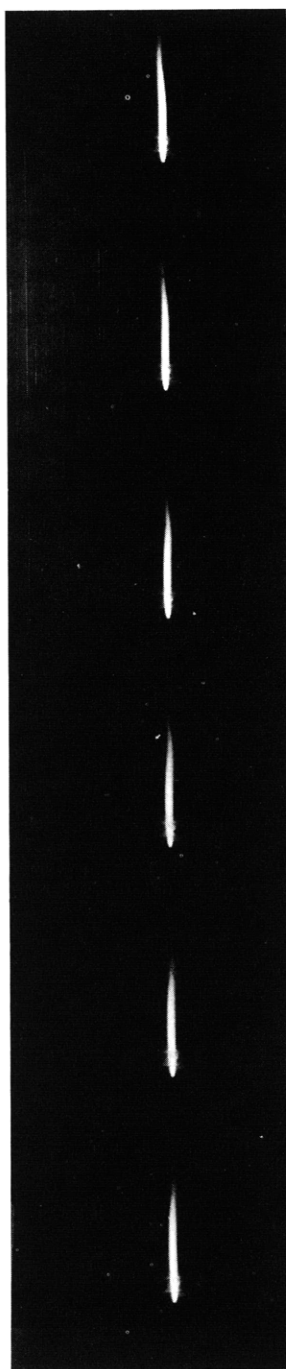
Fig. XII-6. From top to bottom, excited flame with amplifier voltage = 17.5 kv. Excitation and light-chopper frequencies are desynchronized to show the wave propagating up the flame.

the excitation oscillator. The peaks of the waves could then be seen to grow as they traveled through the amplifier section.

Figure XII-5 shows the flame under the following conditions:

$V = 0$

$V_1 = 2.5$ kv

$e_1 = 1.5$ kv peak-to-peak at 30 cps.

Figure XII-6 shows the flame under the same conditions except for V, which was set at 17.5 kv. Notice that a kink can be observed in Fig. XII-6, but that Fig. XII-5 shows no signs of a surface wave. Amplification is not evident from the still pictures, since only one full wavelength is visible, but amplification is obvious in a dynamic experiment in which the phases can be followed.

L. O. Hoppie

References

1. J. R. Melcher, An electrohydrodynamic amplifier, Quarterly Progress Report No. 65, Research Laboratory of Electronics, M.I.T., April 15, 1962, pp. 101-115.

2. L. O. Hoppie, The Electrohydrodynamic Traveling-Wave Amplifier: An Application of Low-Conductivity Plasma, S.B. Thesis, Department of Electrical Engineering, M.I.T., 1962.

3. D. J. Rose and M. Clark, Jr., Plasmas and Controlled Fusion (The M.I.T. Press, Cambridge, Mass., and John Wiley and Sons, Inc., New York, 1961), pp. 258-292.

B. A CRITERION AND AN EXPERIMENT FOR THE OBSERVATION OF ELECTROHYDRODYNAMIC ANTISHOCKS

It has been shown[1] that two types of shocks could form on a free surface flow of a conducting fluid that is stressed by a perpendicular electric field. Within proper energetic constraints, these two types of shock were found to be the regular shock, for which fluid particles propagate from a region of high velocity into a region of low velocity, and the antishock, for which fluid particles propagate from a region of low velocity into a region of high velocity. In this report, the analysis for fully formed surface shocks is extended to indicate a criterion for the formation of antishocks which led to the successful observation of an antishock.

1. Criterion

The pertinent model is shown in Fig. XII-7. By examining energy dissipation and momentum flow, it has been shown[1] that the fully formed shock conditions are:

Regular Shock: $x_2 > x_1$, $\phi_2^2\phi_1^2 > \dfrac{b\epsilon_o V_o^2}{\rho g}$

(1)

Antishock: $x_1 > x_2$, $\phi_1^2\phi_2^2 < \dfrac{b\epsilon_o V_o^2}{\rho g}$.

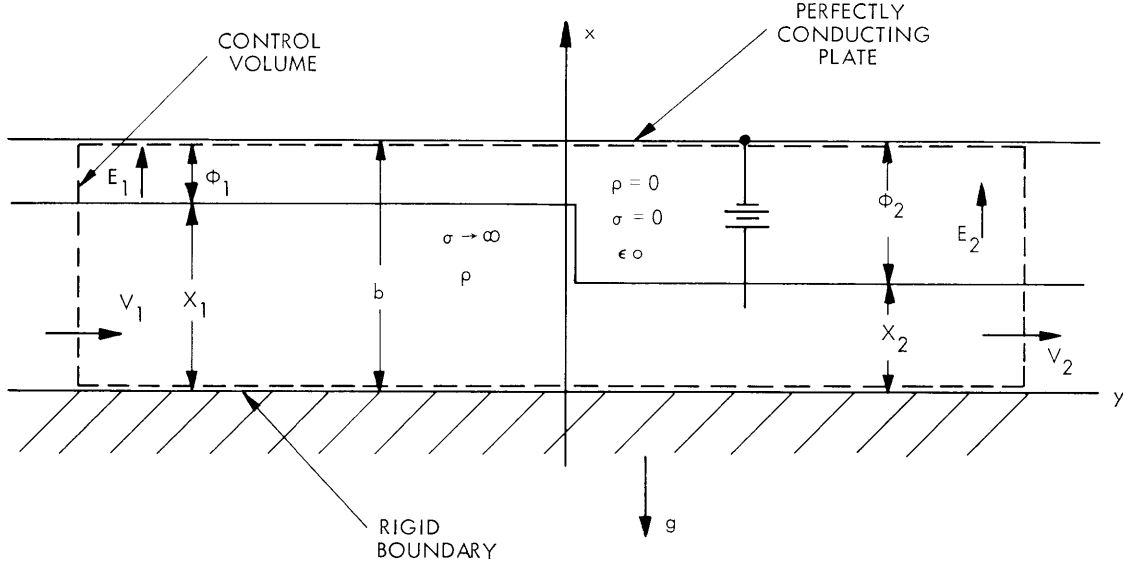For small perturbations on the surface of the flow, the long-wave convective

Fig. XII-7. Definition of model.

dispersion relation is[2]

$$(\omega+\sigma V_1)^2 = \sigma^2\left[gx_1 - \frac{\epsilon_o V_o^2 x_1}{\rho(b-x_1)^3}\right],$$

(2)

where σ is the wave number. Equation 2 implies that the phase velocity of small perturbations with respect to the flow is given by

$$V_{E1}^2 = gx_1 - \frac{\epsilon_o V_o^2 x_1}{\rho\phi_1^3},$$

(3)

and that for the configuration to be stable,

$$x < x_u = b - (\epsilon_o V_o^2/\rho g)^{1/3}.$$

(4)

Using the dimensionless variables, $\eta = x/b$ and $\psi = \phi/b$, and the coupling coefficient,

$K = \epsilon_o V_o^2 / \rho g b^3$, we can rewrite the flow equations[1]

$$q'^2 = q^2(2/b^3 g) = \eta_1 \eta_2 (\eta_1 + \eta_2) - K\eta_1 \eta_2 \frac{(\eta_1 \psi_2 + \eta_2 \psi_1)}{\psi_1^2 \psi_2^2} \tag{5}$$

$$V_1'^2 = V_1^2/bg = q'^2/2\eta_1^2 \qquad V_2'^2 = V_2^2/bg = q'^2/2\eta_2^2 \tag{6}$$

$$\frac{dW'}{dt} = \left[\frac{4\sqrt{2}}{\rho g^{3/2} b^{5/2}} \right] \frac{dW}{dt} = q' \frac{(\eta_2 - \eta_1)^3}{\eta_1 \eta_2} \left[1 - \frac{K}{\psi_1^2 \psi_2^2} \right] \geq 0. \tag{7}$$

The phase velocity and point of instability become

$$V_E'^2 = V_E^2/bg = \eta - K\eta/\psi^3 \tag{8}$$

and

$$\eta_u = x_u/b = 1 - K^{1/3}. \tag{9}$$

The inequality for fully formed regular shock and antishock can be closed in the form

$$\text{Regular Shock:} \quad \eta_2 > \eta_1, \quad \psi_1^2 \psi_2^2 > K, \quad \psi_2^3 > K \tag{10}$$

$$\text{Antishock:} \quad \eta_1 > \eta_2, \quad \psi_1^2 \psi_2^2 < K < \psi_1^3. \tag{11}$$

The coupling coefficient K is the ratio of an electric velocity to a gravity velocity which is evaluated at $x = b$. K has permissible values, $0 \leq K < 1$. $K \to 0$ corresponds to $V_o \to 0$ or $b \to \infty$ or $K = 0$ in the gravity case. $K \geq 1$ corresponds to an unconditional instability.

For an antishock, $\psi_2 > \psi_1$ and $\psi_2^2 \psi_1^2 < K$. With this information and starting from the inequality

$$\psi_1 - \psi_2 < \psi_1 (\psi_1 - \psi_2), \tag{12}$$

we can show[3] that

$$V_1 > V_{E1} \tag{13}$$

or that the front of an antishock must be supercritical. In a like manner the same result can be obtained for a regular shock. For the back of both the regular shock and antishock, it can be shown that

$$V_2 \gtrless V_{E2}, \tag{14}$$

so that the back side flow velocity can be either subcritical or supercritical.

By manipulating a series of arguments that contradict each other, it can be shown[3] that a necessary condition for the formation of an antishock is

$$\eta_1 > \eta_{1t} = 1 - K^{1/4} \tag{15}$$

and that a necessary condition for the formation of a regular shock is

$$\eta_1 < \eta_{1t} = 1 - K^{1/4}. \tag{16}$$

This is exactly the same result that was obtained by a dynamical analysis of this model by ignoring losses.[1] Here, we have accounted for losses in the energetic constraint.
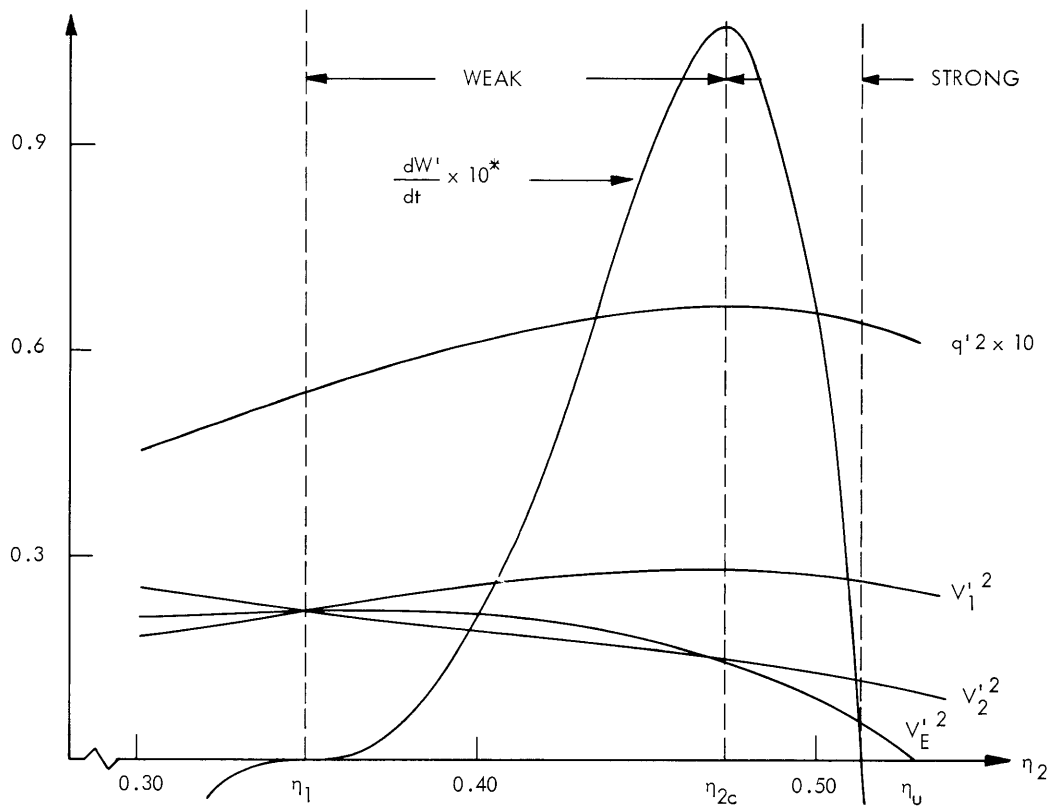

Fig. XII-8. Computed transitions for regular shock (K=0.1).

On the back side, the critical depth, η_{2c}, where $V_{E2} \equiv V_2$ with $\eta_1 \neq \eta_2$, is defined implicitly by

$$\eta_1 + 2\eta_2 - K\frac{(2\eta_2 + \eta_1 - 3\eta_1\eta_2)}{\psi_1^2\psi_2^3} = 0. \tag{17}$$
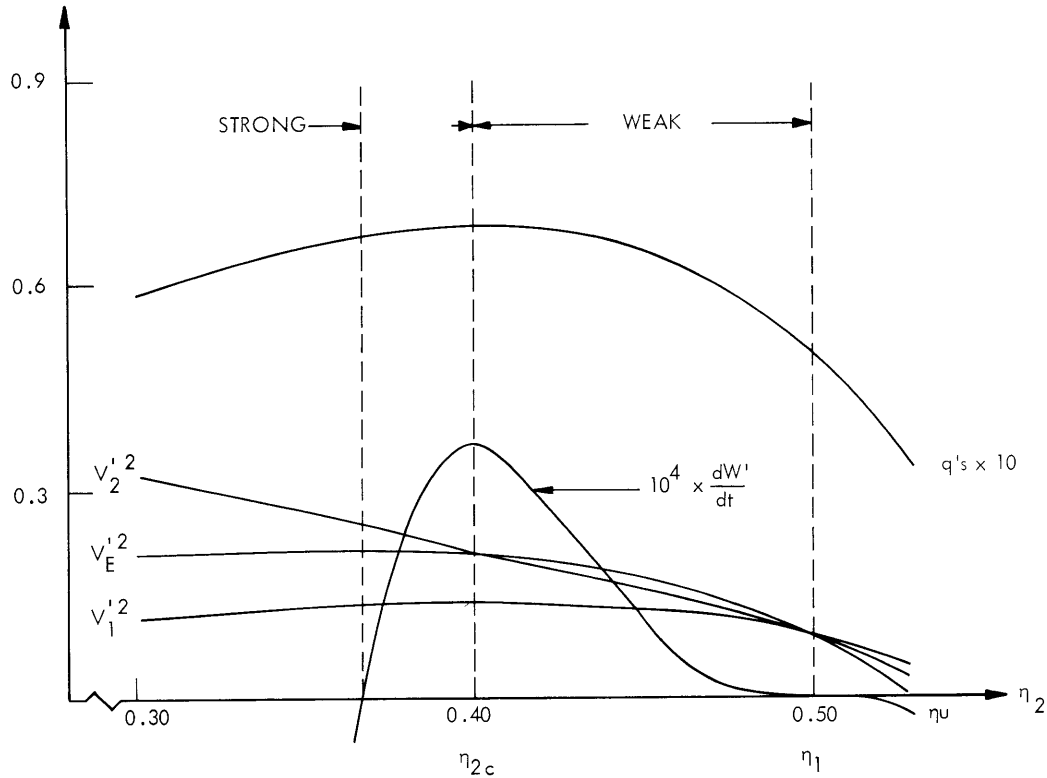
Fig. XII-9. Computed transitions for antishock (K=0.1).

At this critical depth, it can be shown[3] that both q' and dW'/dt have a maximum.

These results are clarified in the computed transitions of Figs. XII-8 and XII-9. In Fig. XII-8, η_1 was chosen to be less than η_{1t} and transitions were computed with dW'/dt > 0 so that regular shock transitions resulted. In Fig. XII-9, $\eta_1 > \eta_{1t}$ and antishock transitions were computed in the valid energy dissipation range. From these curves, there are two possible transitions for each type of shock. The weak shock of both the regular shock and antishock is a supercritical to subcritical transition. The strong shock for both types of shock is the supercritical to supercritical transition. Also, for both types of shock when $\eta_2 = \eta_{2c}$, maximum energy dissipation and flow rate occur.

2. Experiment

The two most difficult problems in observing an electrohydrodynamic antishock are noise on the surface of the fluid and breakdown of the dielectric above the fluid. The noise problem can be minimized by separating η_u and η_{1t} as much as possible. Seeking a maximum of $\eta_u - \eta_{1t}$ yields an optimum value of the coupling coefficient,

$$K_{op} = (3/4)^{12} = 0.031676. \tag{18}$$

177

The maximum E field occurs at the point of instability η_u, where E_{max} is given by

$$E_{max} = V_o/\phi_u = (V_o \rho g/\epsilon_o)^{1/3}.$$ (19)

Between Eqs. 18 and 19, the experiment can be optimized to minimize noise problems and dielectric breakdown.
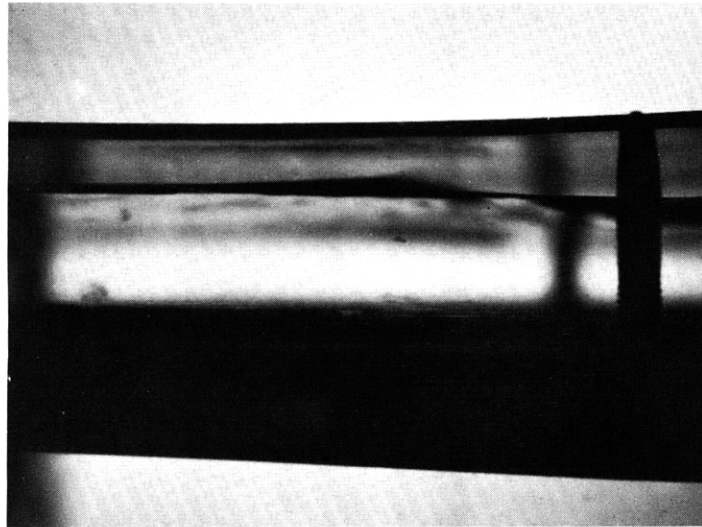

Fig. XII-10.   Fully formed antishock.

For our experiment, water was used as the conducting fluid and air as the dielectric. Various values of coupling coefficient in and around K_{op} were tried, and it was found that, for the purpose of photographs, a spacing of 2 cm and a V_o of 7 kv were best.   A photograph of a fully formed antishock which was made by using these values is shown in Fig. XII-10.   As is visible in the photograph, the plate was curved in order to produce the antishock at this point, stationary in time and space.   It is felt that this is a valid form of excitation as long as the rate of change of the shock front in the y-direction is much greater than the plate variation.

W. H. Childs

References

1.   J. R. Melcher, Magnetohydrodynamic and electrohydrodynamic surface shocks and antishocks, Quarterly Progress Report No. 64, Research Laboratory of Electronics, M.I.T., January 15, 1962, pp. 146-162.

2.   J. R. Melcher, Electrohydrodynamic and magnetohydrodynamic surface waves and instabilities, Phys. Fluids 4, 11(1961).

3.   W. H. Childs, Electrohydrodynamic Shocks and Anti-shocks, S.B. Thesis, Department of Electrical Engineering, M.I.T., June 1962.

C. SPACE-CHARGE DISTRIBUTIONS, INSTABILITIES, AND OSCILLATIONS IN A LOW-PRESSURE DIODE

1. Introduction

We conceive of a parallel plate diode of large extent so that edge effects may be neclected. The hot emitting electrode throws ions and electrons into the diode space. These move in the averaged field that is due to the charged particles in the space and on the electrodes; they do not recombine in the space, but are immediately absorbed upon hitting either collector or emitter. We shall suppose that the kinetic energies of the emitted particles are distributed according to a Maxwell-Boltzmann distribution characterized by the temperature T_e unless we say otherwise.

The basic equations governing the distribution of charges are well known, and the functions resulting from integration of them in the simple case in which only one species of charge is present have been tabulated.[1] There have been extensive investigations[2-5] of the distribution when both ions and electrons are present, but no complete solution has been given. The equations are long and involved; in this report we deal with certain aspects of the solutions and examine as many properties as may be deduced without actually carrying out the integration.

Space-Charge Equations

Figure XII-11 shows the sort of motive diagram that might be considered. The Fermi level of the emitter and collector are shown.

The density of electrons is given by

$$\left.\begin{aligned}
n_e &= n_{oe}\, e^{-\psi}\, \mathrm{erfc}(\psi_m - \psi)^{1/2} \text{ for the range c to e} \\[6pt]
&= n_{oe}\, e^{-\psi}\left(1 + \mathrm{erf}(\psi_m - \psi)^{1/2}\right) \text{ for ranges d to a and b to c} \\[6pt]
&= n_{oe}\, e^{-\psi}\left(1 + \mathrm{erf}(\psi_m - \psi)^{1/2} - 2\,\mathrm{erf}(\psi_a - \psi)^{1/2}\right) \text{ for a to b,}
\end{aligned}\right\} \tag{1}$$

where n_{oe} is the density of the electron stream that is ejected from the emitter. (The actual density of electrons at the emitter is higher if electrons are returned.) $\psi = \dfrac{V_e}{kT_e}$ is a reduced potential.

There is a corresponding equation for the ions. Figure XII-12 is a sketch of the form that these equations take. The letters in this diagram correspond to the letters in Fig. XII-11. It is particularly to be noticed that the density of charge depends only on the potential and the relative positions of potential maxima.

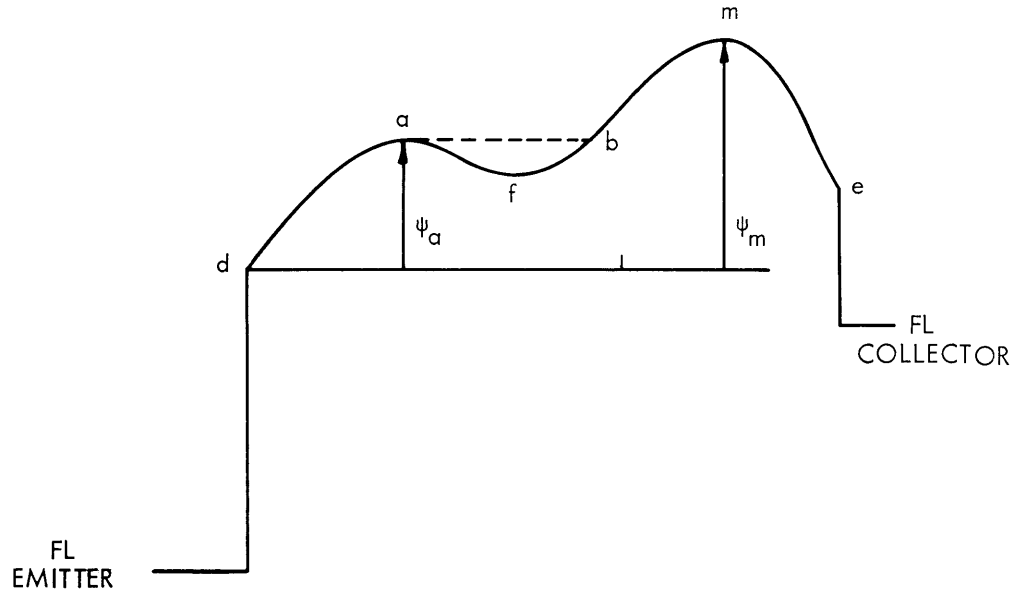The form we devise for Poisson's equation is

179

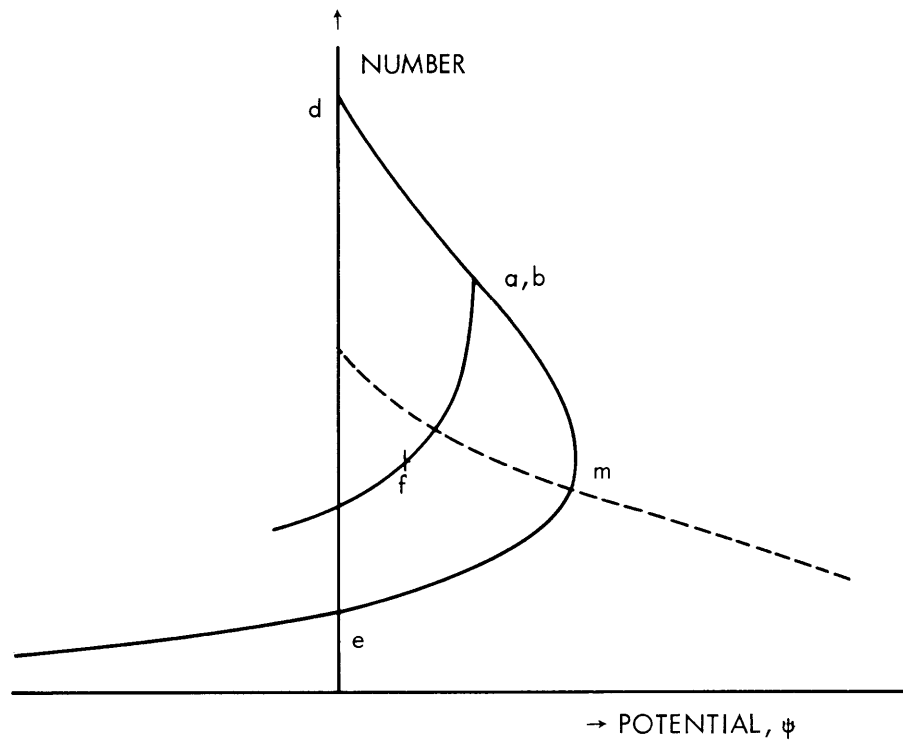Fig. XII-11. Motive diagram for diode.

Fig. XII-12. Variation of density of charge with changes in potential. Dotted curve, which locates the position of the maxima, is for $n = n_0 e^{-\psi}$.

$$\frac{dV}{dx} = \frac{e}{\epsilon_o}\left[\int_{emitter}^{x} n_e dx - \int_{emitter}^{x} n_i dx + C\right],\tag{2}$$

where n_e and n_i are the particle densities and C is the charge on the emitter. This equation brings out (1) that we are considering only the averaged effect of the charges and (2) that in Fig. XII-11 the only charges that affect the field at x are those to the left of a plane passing through x. As a corollary to this, we notice that once the charge on the emitter and its potential are established and the rate of emission of particles and the diode spacing are known, all of the features of the equilibrium charge and potential distributions are determined. Poisson's equation can be reformulated as

$$\left(\frac{\partial V}{\partial x}\right)^2 = \frac{e}{\epsilon_o}\int_{emitter}^{\psi} n_e d\psi - \int_{emitter}^{\psi} n_i d\psi + constant,\tag{3}$$

which is a useful form for some analytical integrations. The solution of the simultaneous equations (1) and (2) constitutes the problem of finding equilibrium conditions.

Finally, the equations can be reduced to the nondimensional form

$$\frac{d^2\psi}{dx^2} = F_e^{(\psi)} - aF_i(\psi),$$

where $F_e(\psi) = n_e/n_{eo}$, $F_i(\psi) = n_i/n_{io}$, $\psi = \frac{eV}{kT}$, $\chi^2 = \frac{x^2}{a^2}$ with $a^2 = \frac{\epsilon_o(kT)^{3/2}\sqrt{2}}{e^2(\pi n_e)^{1/2} i_{eo}}$,

$a = \frac{i_i}{i_e}\sqrt{\frac{n_i}{n_e}}$, and i is the current ejected from the emitter: $i = \sqrt{2kT/\pi m}\, n_o$. Considerations of the curvature of the motive diagram and the way charge depends on potential
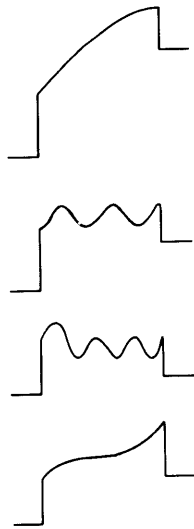

Fig. XII-13. Possible motive diagrams.

181

Fig. XII-14. Impossible motive diagram.

allow certain statements to be made about the form of the possible motive diagrams, especially concerning maxima and minima. If the emitter is on the left of the potential diagram, no maximum less, and only one greater, than a given maximum can be to its left, although there may be many maxima of the same height to the left. The same statement is true if minimum is substituted for maximum. Possible motive diagrams are shown in Fig. XII-13, and an impossible one in Fig. XII-14.

2. Instability and Oscillations

Out of the many possible criteria of stability we choose the following. If a small change of charge on the emitter (and we saw, for given emission rates and diode spacing, that the charge on the emitter completely determines the potential distribution in the space) causes a change in the potential of the collector and in the current flowing through the diode which is such that the outside circuit reacts in a way to aggravate the charge alteration that we made on the emitter, then the potential configuration is unstable.

Furthermore, we wish to point out two kinds of instabilities which we call "general" and "electron" instabilities.

It should be observed that we consider the effect of a change in surface charge only after the effect of the change has reached equilibrium; we assume that it will. This consideration is comparable to a method in the theory of structures in which the structure is given a small displacement, and if the resulting increments in forces on the structure are tending to increase the change, we have an instability. The more sophisticated method of considering the effect of a small oscillatory disturbance and calculating the attenuation of its effects is not considered, and would be unnecessarily complicated.

General instability arises from the consideration that the whole distribution of positively and negatively charged particles is altered by the change in charge. But if we suppose that the ion distribution is fixed and that only the electron distribution and, of course, the potential distribution are altered, then it may be that this supposition shows us a second sort of instability — electron instability. This instability is interesting, since it is certain that the electrons in most cases that we consider are many times more mobile than the ions, and it seems a reasonable physical approximation to suppose that if the electrons have two distributions for a given distribution of ions, then they will take on the more stable distribution. If this state does not happen to be a general equilibrium state, then the ions will begin to redistribute themselves. An oscillatory condition is envisaged. By beginning from a general equilibrium state, if the
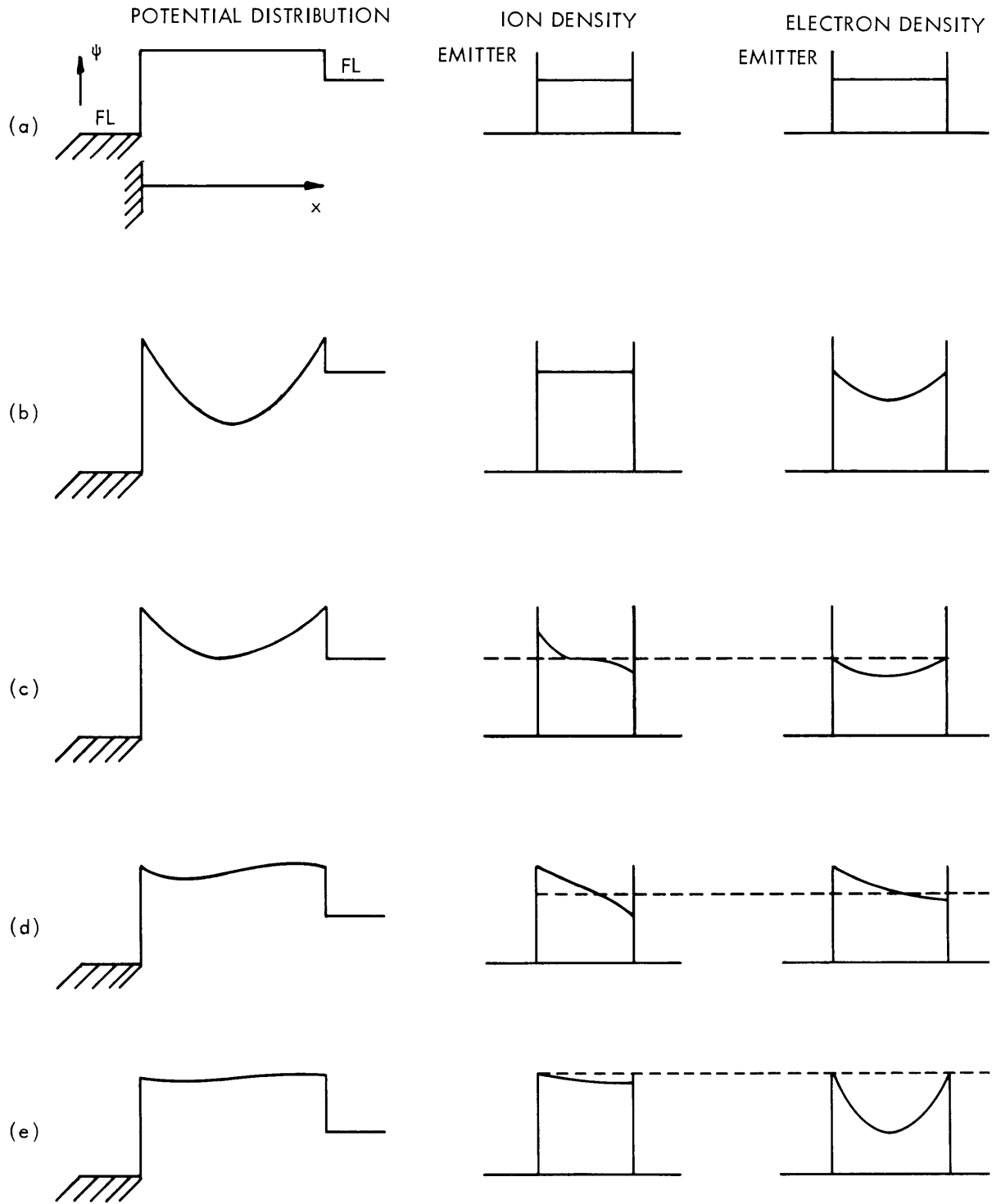
POTENTIAL DISTRIBUTION   ION DENSITY   ELECTRON DENSITY

Fig. XII-15. Initial and subsequent potential, electron, and ion density distributions.

electrons have another different equilibrium distribution for this distribution of ions
which is more stable, we consider them to assume it directly. The ions now move, and
probably the potential relaxes, as it were, toward the original equilibrium state. But
at some stage in this relaxation the electrons again have two states of equilibrium, one
stable, and they will take up this stable state. The ions again adjust their distribution.
The calculation suggested considers the electron distribution to be always in equilibrium
with the potential distribution and the ions never to be so.

EXAMPLE: The mathematics of this subject is extremely complicated. There seems
to be no analytic solutions even for the steady state. But, again without actually doing
any computations, we can understand something of the phenomena in a qualitative way.

Consider the simple case in which we have ions and electrons being emitted so that
the net space-charge density at the emitter is zero in the emitted beam, but not zero at
the emitter surface if some charges are returned to the emitter. Consider, further-
more, the case in which a battery is connected to the outside circuit so that the surface
potentials of collector and emitter are equal. The potential, ion, and electron distribu-
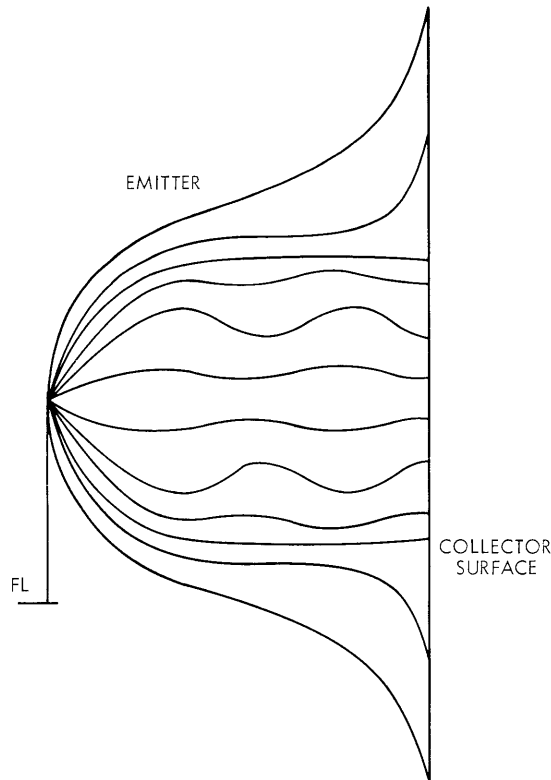tions are shown in Fig. XII-15, on the top line. (In Fig. XII-16 are shown other

Fig. XII-16. Potential distributions for equal densities in emitted
beams of ions and electrons.

equilibrium distributions of potential. It is unclear how or where the oscillatory — these are space waves — solutions cross.)

Now consider general stability. The effect of placing a charge on the emitter is to alter the gradient of the potential diagram at the emitter. Examination of the curvature shows that none of the oscillatory solutions in Fig. XII-16 cross the line of zero potential, so that the potential of the collector increases as we increase the slope of the potential diagram at the emitter, and decreases if we decrease it. The battery reacts to an increase in charge on the emitter by removing charge so that the slope is reduced. The charge corrects itself, as it does if we consider a decrease in charge on the emitter; the distribution is generally stable.

But consider electron instability. Let x_o be the spacing of the diode in dimensionless units. $n_i = n_{io}$ = constant.

If a slight increase in slope is considered, although near the emitter, there may be a net negative space charge; the potential can never go through a maximum, since at any supposed maximum there is always a net positive space charge that is quite incompatible with a maximum. (A glance at Fig. XII-12 will make this clear.)

But if we consider a decrease in slope and suppose that the potential curve does not come above zero potential, then

$$\text{the net charge} = n_{io} - n_{eo}\, e^{-\psi}(1 - \mathrm{erf}(-\psi)^{1/2})$$

$$\doteq -n_{io}\frac{2\psi^{-1/2}}{\sqrt{\pi}} \text{ for small } \psi$$

$$= \frac{d^2\psi}{dX^2}$$

$$\therefore \frac{d\psi}{dX} = K_2 - \frac{4n_{io}}{3\sqrt{\pi}}\,\psi^{3/2}.$$

The constant, K_2, is small and is a measure of the initial change in slope. For some small ψ which is of the order of K_2, $\frac{d\psi}{dX} = 0$ and, since the potential curve is symmetric about the minimum, if the distance to this minimum is also of the order of K_2, the curve must meet the zero-potential line again. Once it is shown that the potential must pass through zero, then the argument given above applies and we have established that the potential at the collector is above zero potential. The battery, to correct this, puts charge on the emitter, and thus the slope at the emitter is decreased. The situation is aggravated and we have an instability.

The distance from the emitter to the minimum is

$$\int_0^{X_m} dX = \int_0^{\psi_m} \frac{d\psi}{\left| \left\{ K_2 - K_1 \psi^{3/2} \right\} \right|}; \quad K_1 = \frac{n_{io}^4}{3\sqrt{\pi}} \doteq \frac{6}{5} K_1^{2/3} K_2^{1/6}.$$

This distance is of the order of K_2 and, therefore, is small. Hence, the potential curve will cross the zero line and our initial assumption that the potential does not pass zero was wrong: the distribution is indeed unstable.

The new distribution of electrons is illustrated in line b of Fig. XII-15. The ions are certainly not in equilibrium in this potential field, but their subsequent redistribution is unclear and the subject of further investigation. A speculation about this redistribution is shown in lines c, d, and e of Fig. XII-15. Line e again exhibits electron instability, and it is supposed that this sort of state will be continually reappearing with a relaxation between appearances. The mathematics is very complex, but it seems that the simplification, by allowing the injected ions to be monoenergetic, may permit an easier calculation. In any event, only an approximate solution seems possible.

But what we have established is that under certain circumstances, of which we have cited an example but whose range is not yet circumscribed, we have only one general equilibrium solution, which is, in fact, unstable. We have also outlined a possible mode of oscillation.

W. T. Norris

References

1. W. B. Nottingham, Technical Report No. 321, Research Laboratory of Electronics, M.I.T., December 10, 1956.

2. P. L. Auer, J. Appl. Phys. **31**, 2096 (1960).

3. P. L. Auer and H. Hurwitz, J. Appl. Phys. **30**, 161 (1959).

4. A. L. Eichenbaum and K. G. Hernqvist, J. Appl. Phys. **32**, 16 (1961).

5. I. Langmuir, Phys. Rev. **33**, 954 (1929).